Cerebral Cortex February 2009;19:445–454
doi:10.1093/cercor/bhn095
Advance Access publication June 11, 2008

Striatal Dopamine and Working Memory

Susan M. Landau[1,2], Rayhan Lal[1], James P. O'Neil[2], Suzanne Baker[2] and William J. Jagust[1,2]

[1]Helen Wills Neuroscience Institute, University of California, Berkeley, CA 94720-3190, USA and [2]Lawrence Berkeley National Laboratory, Department of Functional Imaging, Berkeley, CA 94720, USA

Recent studies have emphasized the importance of dopamine projections to the prefrontal cortex (PFC) for working memory (WM) function, although this system has rarely been studied in humans in vivo. However, dopamine and PFC activity can be directly measured with positron emission tomography (PET) and functional magnetic resonance imaging (fMRI), respectively. In this study, we examined WM capacity, dopamine, and PFC function in healthy older participants in order to test the hypothesis that there is a relationship between these 3 factors. We used the PET tracer 6-[^{18}F]fluoro-L-*m*-tyrosine to measure dopamine synthesis capacity in the striatum (caudate, putamen), and event-related fMRI to measure brain activation during different epochs (cue, delay, probe) of a WM task. Caudate (but not putamen) dopamine correlated positively with WM capacity, whereas putamen (but not caudate) dopamine correlated positively with motor speed. In addition, delay-related fMRI activation in a left inferior prefrontal region was related to both caudate dopamine and task accuracy, suggesting that this may be a critical site for the integration of WM maintenance processes. These results provide new evidence that striatal dopaminergic function is related to PFC-dependent functions, particularly brain activation and behavioral performance during WM tasks.

Keywords: aging, caudate, fMRI, maintenance, PET, putamen

Introduction

Working memory (WM) is the set of cognitive and neural processes involved in holding information in mind for later use (Baddeley 1992), and it is critical for carrying out many everyday tasks. A substantial body of evidence supports roles for both prefrontal cortex (PFC) and dopaminergic neurotransmission in normal WM function (Cools and Robbins 2004). During the delay epoch of WM tasks, maintenance processes make it possible to hold information in mind in the absence of external stimuli. This period, in particular, appears to engage the dopamine system in the PFC (Williams and Goldman-Rakic 1995; Floresco and Phillips 2001) through a cyclic adenosine monophosphate and D1 receptor mediated process in which low levels of dopamine improve spatial tuning of PFC neurons, whereas high levels of dopamine impair tuning (Vijayraghavan et al. 2007). A variety of factors related to variability in dopamine function may thus underlie behavioral performance on WM tasks. It has been hypothesized that WM capacity, in particular, is associated with dopaminergic variability (Salthouse et al. 1991; Kimberg et al. 1997; Kimberg et al. 2001). Although the mesocortical circuit is the source of direct dopaminergic input to the PFC, influencing neural function and behavior, it has also been proposed that nondopaminergic inputs to the PFC from the caudate (via basal ganglia–thalamocortical loops) (Alexander et al. 1986) may be critically involved as well, a theory supported by the involvement of the caudate in WM tasks (Lewis et al. 2004) as well as studies of WM in patients with Parkinson's disease (PD; Owen et al. 1998).

The hypothesized associations between dopamine function and WM capacity (Kimberg et al. 2001) are based on inferences, rather than direct measurements, of endogenous dopamine markers. However, direct measurement of dopamine (DA) function in humans is possible with positron emission tomography (PET) and a number of different ligands for presynaptic DA synthesis capacity, DA transporters, vesicular transporters and dopamine receptors. In this study, we utilized the tracer 6-[^{18}F]fluoro-L-*m*-tyrosine (FMT) which is a good substrate for aromatic amino acid decarboxylase (AADC) thus providing a method of assaying the synthesis capacity of DA neurons in the densely DA-innervated striatum (DeJesus et al. 1997; Jordan et al. 1997).

In this study, our goal was to relate DA synthesis capacity (measured with FMT-PET) to event-related brain activation (measured with functional magnetic resonance imaging [fMRI]) during performance of a WM task as an index of brain activation. We were specifically interested in evaluating relationships between dopaminergic function, WM capacity, and load-related activation in the PFC, based on the known neural circuits (Alexander and Crutcher 1990; Middleton and Strick 2000) and the substantial evidence linking caudate activation, dopamine, and WM (Volkow et al. 1998; Kimberg et al. 2001; Carbon et al. 2004; Chang et al. 2007; Cools et al. 2008). We were also interested in examining possible differences in caudate and putamen dopamine, based on the hypothesis that the putamen is disproportionately involved in motor processing, whereas the caudate is primarily involved in cognitive function (Bhatia and Marsden 1994; Rinne et al. 2000). Finally, we studied healthy older individuals because normal aging is associated with increased individual differences in WM performance, brain activation (Reuter-Lorenz and Lustig 2005), and dopamine function (Backman et al. 2000; Erixon-Lindroth et al. 2005), so this group was likely to provide sufficient variability to identify correlational relationships between these factors.

Materials and Methods

Participants

23 healthy older right-handed participants (5 males; mean age = 67.1 ± 7.4; mean years of education = 17.9 ± 3.3;) were recruited from the Berkeley Aging Cohort, a database of healthy older participants living in Berkeley and the surrounding community. Inclusion criteria for participation were 1) age between 55 and 85 years, 2) Mini-Mental State Examination (MMSE) score $\geq$ 26, 3) normal cognitive function as

judged by a neuropsychological test battery, 4) absence of depression based on a score < 6 on the Geriatric Depression Scale (Yesavage et al. 1982–1983). Exclusion criteria were 1) cognitive impairment or dementia, 2) evidence of significant brain disease, including history of stroke or evidence on structural MRI of stroke, excessive atrophy, or significant white matter hyperintensity, 3) history of substance abuse, use of any medications with central nervous system effects, 4) psychiatric illness, 5) hypertension, diabetes, or other systemic medical illness, 6) contraindications to MRI or PET including pacemaker, metallic implants, claustrophobia, or history of radiation therapy, 7) presence of parkinsonian symptoms based on the Unified Parkinson's Disease Rating Scale (Fahn and Elton 1987) which was performed by a neurologist (W.J.J.).

All participants gave written, informed consent prior to participation in the study. All subjects completed one neuropsychological testing session and 2 imaging sessions, with the exception of one individual whose PET session data was omitted due to excessive motion (>6 mm). Behavioral data during fMRI scanning was lost for that individual as well due to technical problems, but the fMRI data for that individual is intact and is included in the first-level mapwise fMRI analysis.

Behavioral Testing and Analysis

A neuropsychological battery was given during an initial session within 2 months of the fMRI and PET scans in order to obtain measures of 1) global cognitive ability, to ensure normal cognitive function, 2) WM function, 3) motor speed. Correlations (Pearson's R) were conducted between these neuropsychological test measures and the PET region of interest (ROI) measures (see PET methods below) at $P < 0.05$.

Tests of global cognitive ability included the MMSE (Folstein et al. 1975) and several subtests of the Wechsler Adult Intelligence Scale—Revised (Wechsler 1987).

Two WM performance measures were used to test our hypothesis that WM performance (but not global cognitive ability) was related to dopamine function. First, WM capacity was measured using the Salthouse and Babcock Listening Span task (Salthouse et al. 1991). Briefly, this test requires participants to listen to the experimenter read sets of consecutive unrelated sentences (e.g., "After dinner, the chef prepared dessert for her guests") that increase in number from 1 to 7. There are 3 trials at each the 7 levels, for a total score of 84 possible correct words. During each trial, the participant is asked to listen to the sentences while checking boxes in response to comprehension questions they read simultaneously, then turn the page and write the final word from each sentence in the correct order. Our WM capacity measure was the total number of words recalled across all 7 levels of this test.

The second WM measure was mean reaction times (RTs) for correct trials and accuracy for low load trials (2 letters), and high-load trials (6 letters) of the Sternberg delayed recognition task (Sternberg 1966), performed during the fMRI scanning session (see fMRI Behavioral Methods). Accuracy scores were highly positively skewed (mean percent trials correct = 93.2 ± 9.9%) and were corrected using an arcsine transformation (x = arcsin(sqrt(n)). Finally, motor speed was measured with the simple RT (zero load) condition of the Sternberg task.

Planned linear regressions between dopamine ROI K_i and behavioral measures were carried out at $P < 0.05$, 2 tailed.

PET Methods

The tracer FMT is a substrate for AADC and thus reflects the capacity of the aggregate dopaminergic neurons to synthesize dopamine, providing a measure of presynaptic dopamine function. Metabolism of FMT by AAAD produces 6-[^{18}F]fluorometatyramine (FMA). FMA is rapidly oxidized to 6-[^{18}F]fluorohydroxyphenylacetic acid which remains trapped in the striatum and is responsible for most of the radioactive signal in the PET image. FMT-PET scans thus reflect uptake and AAAD activity (Jordan et al. 1997; DeJesus 2003). FMT was synthesized at the Lawrence Berkeley National Laboratory with a modification of the procedure described previously (Namavari et al. 1993).

PET scans were performed using the Siemens (Knoxville, TN) ECAT EXACT HR PET scanner in 3D acquisition mode. This instrument was designed with a 3.6-mm in-plane spatial resolution and 47 parallel imaging planes, with retractable septae for 3D imaging.

All participants were studied starting at approximately 60 min after an oral dose of 2.5 mg/kg of carbidopa. Participants were positioned on the scanner bed with a pillow and padding to comfortably restrict head motion. A 10-min transmission scan was obtained for attenuation correction, then approximately 3 mCi of FMT was subsequently injected as a bolus in an antecubital vein and a dynamic acquisition sequence in 3D mode was obtained: 4 × 1 min, 3 × 2 min, 3 × 3 min, 14 × 5 min for a total of 89 min of scan time.

Data were reconstructed using an ordered subset expectation maximization algorithm with weighted attenuation, an image size of 256 × 256, and 6 iterations with 16 subsets. A Gaussian filter with 6-mm full width half maximum (FWHM) was applied, with a scatter correction. Images were evaluated for subject motion and adequacy of statistical counts.

PET Data Analysis

Following the scanning session, PET data were realigned to the mean image of the first 10 frames. Motion between time-series frames was then corrected using algorithms implemented in Statistical Parametric Mapping (SPM2; Wellcome Department of Imaging Neuroscience, UK). PET data were then coregistered to each individual's high-resolution magnetization-prepared fast low angle shot (MP-FLASH) (0.875 × 0.875 × 1.54 mm) obtained during the fMRI session for each subject (see below) using a 12-parameter affine algorithm implemented in SPM2. This permitted the use of the high-resolution MRI image for anatomical definition of PET ROIs.

K_i values, representing the overall uptake rate constant that quantifies tracer uptake across a ROI, were calculated using a graphical analysis method for quantification of brain uptake of irreversible ligands (Patlak and Blasberg 1985). A simplified reference tissue method was used, thus omitting need for arterial blood sampling (Lammertsma and Hume 1996). Bilateral cerebellar ROIs were drawn on consecutive 1.54-mm slices of the high-resolution MR image and used as the reference tissue. Use of this reference tissue method in actuality does not produce a true K_i that indicates net tracer uptake, but rather a value of K_i which is scaled to the volume of distribution of the tracer in the reference tissue. We use the term K_i for simplicity.

In order to test hypotheses about dopamine differences in subregions of the striatum, we defined ROIs in the right and left caudate and putamen. An axial image representing the sum of the last 4 emission scans of the PET scanning session (4 × 5 min frames) was coregistered to the high-resolution MR scan. ROIs were drawn on these images (Wang et al. 1996; Volkow et al. 1998), using the MR scan and the atlas of Talairach as references. ROIs were drawn on data in native space in order to preserve differences in tracer uptake due to anatomical variability between subjects. We have previously demonstrated the ability to draw ROIs with high inter-rater reliability (Klein et al. 1997). The Patlak model was fitted with dynamic data from each ROI from 24 to 89 min, when the regression is highly linear ($R > 0.99$). For 3 subjects, the last 3 frames (75–89 min) were truncated due to nonlinearities in the Patlak model that were introduced due to motion.

K_i values for right and left portions of the caudate and putamen were highly correlated across individuals, so they were averaged together for subsequent analyses to reduce the number of statistical tests. Caudate and putamen K_i were also highly correlated, but they were not aggregated because of our a priori hypotheses that distinct cognitive and motor functions that may be subserved by dopamine in the caudate and putamen (Rinne et al. 2000).

PET Voxelwise Correlational Analyses

To prepare voxelwise K_i volumes in a common space across subjects, each voxelwise K_i volume in native space was spatially normalized to a custom template that was created using the minimum deformation method of Kochunov et al. (2001) that was implemented using SPM2 spatial normalization. Briefly, this template was created as follows: First, K_i volumes were coregistered to each subject's high-resolution MR volume; second, an arbitrary MR volume was coregistered to Montreal Neurological Institute (MNI) template space; second, the other MR volumes were coregistered to this arbitrary volume; third, the K_i volume that minimized deformations for all other K_i volumes was identified and mean deformations were applied to it. This interpolated

volume served as the final template. All MR volumes were normalized to the template, and the normalization parameters were applied to each subject's K_i volume.

Voxelwise linear regressions were carried out with these K_i volumes and subjects' test scores for the neuropsychological measures listed in Table 1 (Listening Span Test, Vocabulary, Arithmetic, motor speed) at $P < 0.001$ (2 tailed), uncorrected. A 15 voxel extent threshold was used rather than the clusterwise correction applied to the fMRI data because we anticipated finding relatively small clusters within the striatum, the predominant site of FMT uptake.

fMRI Imaging Methods

fMRI experiments were performed at the Henry H. Wheeler, Jr, Brain Imaging Center with a Varian Unity/Inova whole body 4.0T scanner (Palo Alto, CA; www.varianinc.com) with a transverse electromagnetic send-and-receive head coil (MR Instruments, Minneapolis, MN; www.mrinstruments.com).

The imaging session lasted approximately 70 min, and consisted of acquisition of anatomical and functional images. Two T_1-weighted anatomical scans were acquired. The first was coplanar with the echoplanar imaging (EPI) data and was collected using a gradient-echo multislice sequence (time repetition [TR] = 200 ms, time echo [TE] = 5 ms, field of view [FOV] = 22.4 cm^2, matrix size = 256 × 256, in-plane resolution = 0.875 × 0.875). The second was a high-resolution anatomical scan for use in ROI drawing, intersubject coregistration, and normalization to the MNI reference brain. This scan was acquired with an MP-FLASH 3D sequence (TR = 9 ms, TE = 5 ms, FOV = 22.4 × 22.4 × 19.8 cm, matrix size = 256 × 256 × 128, resolution = 0.875 × 0.875 × 1.54 mm).

Functional imaging consisted of 2-shot gradient-echo EPI images acquired for 18 axial slices with a FOV of 22.4 cm, flip angle of 20°, 3.5 mm × 3.5 mm in-plane voxel size with 5-mm slice thickness and a 1-mm gap for full brain coverage, and a 64 X 64 matrix. Functional scans were conducted with TR = 2000 ms and TE = 28 ms.

Letter stimuli for the delayed recognition task were presented using E-Prime (Psychology Software Tools, Pittsburgh, PA) during continuous scanning. Participants viewed stimuli in the scanner via back-projection onto a custom designed nonmagnetic screen mounted at the participant's chest level, which was viewed using an angled mirror placed inside the head coil. Participants responded to stimuli presented on the screen by making yes/no key-presses on a nonmagnetic response box designed for use in the scanner. Prior to scanning, participants with poor visual acuity were fitted with nonmagnetic corrective lenses.

fMRI Behavioral Methods

Subjects performed a version of the Sternberg delayed recognition task using letter stimuli (Sternberg 1966; Rypma et al. 2002; Gibbs and D'Esposito 2005) during the fMRI scanning session. Prior to scanning, participants completed a practice run of 15 trials on a computer in order to familiarize them with the task.

Each trial of the Sternberg delayed recognition task consisted of cue (4 s), delay (12 s), and probe (2 s) epochs. During the cue, 2, 4, or 6 block capital letters were presented, followed by an unfilled delay. Following the delay, a single lowercase probe letter appeared, and participants were instructed to indicate whether the probe letter was a part of the set presented during the cue with a manual button-press (right = yes; left = no). A lowercase letter was used for the probe in order to prevent retrieval from the encoding set based on perceptual features alone. The probe was followed by a jittered intertrial interval lasting between 8 and 12 s. Five trials of each of the 3 types were presented per 7-min run. There were 6 runs, for a total of 90 trials per scanning session. The 3 memory loads were counterbalanced across each scanning run and across the session.

At the end of the scanning session, when the high-resolution image was being acquired (but no functional data), subjects performed 15 trials of a "zero load" condition of the delayed recognition task in order to measure RT under conditions when WM load did not contribute to RT. These trials were identical to the 2, 4, and 6 load conditions, except that the letter stimuli were replaced with 4 Xs during the cue and with a single "X" during the probe, and only behavioral data was acquired in order to measure simple motor speed. Subjects were instructed to press *both* right and left buttons when they saw the single "X" presented during the probe epoch.

fMRI Statistical Analyses

Functional images acquired from the scanner were reconstructed offline from k-space. Image volumes were corrected for slice timing skew using temporal sync-interpolation and corrected for movement using rigid-body transformation parameters. Image preprocessing and statistical analyses were performed using SPM2 (www.fil.ion.ucl.ac.uk/spm). Images were smoothed with a 7-mm FWHM Gaussian kernel. A high-pass filter was used to remove frequencies below 0.01 Hz from the data.

Data were analyzed using the general linear model (GLM) (Worsley and Friston 1995). For each subject, the blood oxygen level–dependent (BOLD) signal for each task epoch (cue, delay, and probe) and for each trial type (low load, 2 letters; medium load, 4 letters; high load, 6 letters) were modeled as impulses of neural activity convolved with the SPM canonical hemodynamic response function relative to the fixation epoch. Covariates were entered into the GLM according to the following structure: the first covariate was at the onset of the cue epoch (first TR, 0 s), modeling encoding processes during the cue epoch. A second covariate at the third TR (4 s) modeled late cue-related activity. Because late encoding processes may continue into the delay, this late cue covariate was modeled to reduce noise in the estimate of the baseline, but was not included in contrasts used to define ROIs (Zarahn et al. 1999). The early and late phases of the delay epoch were modeled with covariates at the fifth and seventh TRs, respectively (8 and 12 s), associated with maintenance processing. The delay effects reported here represent the sum of the 2 delay covariates. The probe epoch was modeled with a covariate at the onset of the probe (ninth TR, 16 s), associated with memory retrieval.

In order to restrict our analyses to activation related to accurate performance (correct trials only), we modeled incorrect trials using a separate covariate which was not included in the subsequent contrasts outlined below. In order to examine brain activation related to increased WM demand, rather than primary sensory or motor processing, individual contrast maps of regions with greater activation at higher WM loads were then generated with the contrast [−1, 0, +1] (low load, 2 letters; medium load, 4 letters; high load, 6 letters) for each task epoch (cue, delay, probe).

Finally, each participant's brain was normalized to the MNI reference brain using SPM2. Spatial normalization was then performed as a 2-step procedure: first, the high-resolution MP-FLASH anatomical structural image was coregistered to the structural image in-plane with the EPI images using SPM2. Second, the MP-FLASH image was spatially normalized using SPM2. The resulting transformation was used to spatially normalize the individual contrast maps.

Table 1

Caudate and putamen dopamine function correlate with distinct behavioral indices

	Dopamine synthesis			
	Caudate		Putamen	
	R	*P*	*R*	*P*
Neuropsychological measures				
Listening span	**0.45**	**0.04**	0.34	0.12
Vocabulary	−0.10	0.97	0.06	0.79
Arithmetic	−0.06	0.81	0.18	0.44
Sternberg task performance				
RT—zero load/simple RT only	−0.12	0.60	**−0.45**	**0.05**
RT—low load trials	0.13	0.57	0.01	0.96
RT—high-load trials	0.30	0.18	0.20	0.38
Accuracy—low-load trials	0.13	0.56	0.22	0.34
Accuracy—high-load trials	**0.39**	**0.08**	0.29	0.19

Note: Pearson's correlation coefficients (R) are shown for relationships between behavioral data (neuropsychological test measures, behavioral measures from the Sternberg task performed during fMRI scanning) and K_i values reflecting dopamine synthesis capacity in caudate and putamen. Sternberg delayed recognition task performance measures include mean accuracy and RT for low (2 letters) high (6 letters) WM loads.

fMRI Random-Effects Analyses

Random-effects analyses were performed using normalized load-sensitive contrast maps in order to identify regions for each task epoch (cue, delay, probe) that showed increased activation with increased WM load. Delineation of regions with increased activation corresponding to increased load within the map was performed based on a peak statistical threshold of $P < 0.001$ (1 tailed, $t = 3.55$), and cluster size of 54 voxels within the same anatomical region of the peak as defined by the MNI anatomical template. This resulted in an overall statistical threshold of $P < 0.05$, cluster corrected (Cao 1999).

fMRI Voxelwise Correlational Analyses

Voxelwise linear regressions was carried out at $P < 0.001$ (2 tailed), uncorrected, in order to identify regions where load-sensitive activation at each trial epoch (cue, delay probe) correlated with PET ROI measures (caudate and putamen K_i) across participants. The search volume was restricted for these analyses within the load-sensitive contrast map identified above. All coordinates of voxelwise analysis results are reported with respect to the MNI atlas.

Results

Behavioral Analyses

Participants had a mean MMSE score of 29.4 (±1.0) indicating normal global cognitive function. The total number of words recalled for the Listening Span Test ranged from 35 to 70 (mean 50.9 ± 9.1). Mean vocabulary and arithmetic scores were 58.2 ± 5.4, and 16.3 ± 3.4, respectively. On the Sternberg recognition task, subjects showed increased RT with increasing WM load and performed the task with high levels of accuracy (mean accuracy = 93.2 ± 9.9).

PET Voxelwise Analysis

Linear regression was conducted on the voxelwise PET volumes using the neuropsychological measures listed in Table 1 as covariates. This analysis revealed that K_i in bilateral regions in the dorsomedial portion of the caudate was related to WM capacity across individuals (see Fig. 1). There were no significant voxels that resulted from correlations with vocabulary or arithmetic scores.

PET ROI Analysis

Across individuals, caudate ROI K_i values ranged from 0.0162 to 0.0240 (mean = 0.0201 ± 0.0023). Putamen ROI K_i ranged from 0.0164 to 0.0255 (mean = 0.0214 ± 0.0024). Putamen K_i values were higher than caudate K_i values ($P < 0.001$, 2 tailed).

Regression analyses between behavioral measures (neuropsychological test and Sternberg task data) and caudate and putamen ROI K_i values are listed in Table 1.

With respect to the neuropsychological measures, Caudate K_i values showed a positive correlation with WM capacity (Listening Span Test) ($R = 0.45$, $P = 0.04$) and a marginal correlation with Sternberg task accuracy for high-load (but not low load) trials ($R = 0.39$; $P = 0.08$).

Putamen K_i values did not correlate with any of the cognitive neuropsychological measures, but putamen did correlate negatively with simple RT (zero load trials on the Sternberg task; $R = -0.45$; $P = 0.05$, 2 tailed; Table 1), indicating that faster motor speed was associated with higher putamen dopamine function. Caudate K_i values showed no relationship to motor speed.

Finally, age did not correlate with caudate or putamen K_i values. Age did correlate negatively with Listening Span test performance ($R = -0.43$, $P = 0.04$), but effects of age were not significant for other neuropsychological measures ($P > 0.10$). Because of the correlation between age and Listening Span test performance, we performed a follow-up analysis, partialling out the effect of age in the significant relationship between Listening Span test performance and caudate ROI K_i (shown in Table 1). The positive correlation between Listening Span test performance and caudate ROI K_i remained significant ($R = 0.54$, $P = 0.01$) after accounting for age.

Load-Sensitive Brain Activation

The fMRI random-effects analysis identified a number of brain regions showing significantly greater activation with increased WM load during performance of the delayed recognition task (see Fig. 2 and Table 2). Overall, we observed load-related activation across a bilateral network of prefrontal, premotor, motor, parietal, and visual regions during the cue and delay epochs, but only one region (in the left middle frontal gyrus) during the probe.

During the cue epoch, there was increased load-sensitive activation in bilateral middle frontal gyri, inferior frontal gyri, precentral gyri, supplementary motor area, superior and inferior parietal lobules, occipital cortex, caudate, putamen,

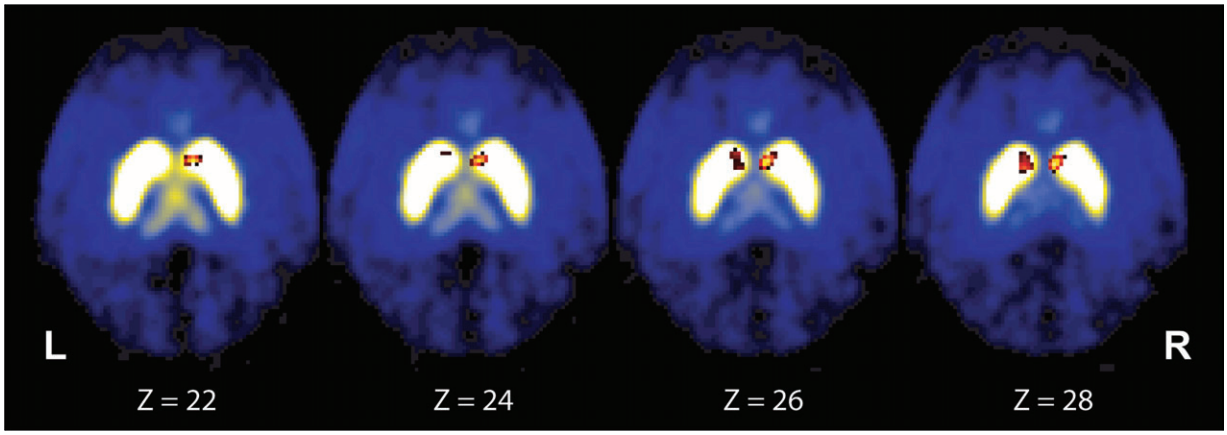

Figure 1. Dopamine synthesis correlates with WM capacity. A voxelwise regression on K_i values and total words recalled on the Listening Span Test revealed that individuals with higher bilateral caudate dopamine scored higher on the Listening Span Test.

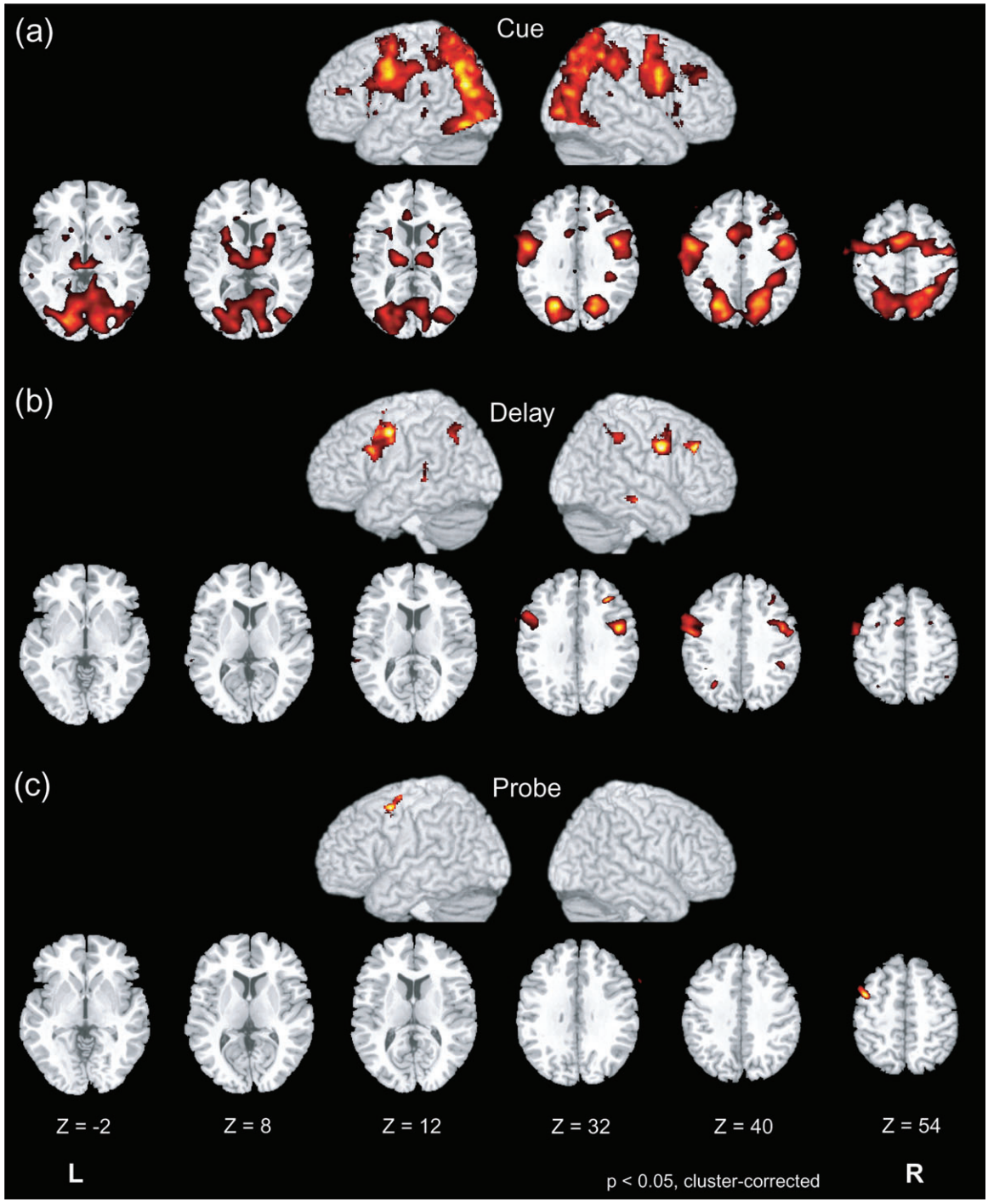

Figure 2. Increased WM load is associated with increased brain activation in a number of regions during the (*a*) cue, (*b*) delay, and (*c*) probe epochs of the Sternberg delayed recognition task ($P < 0.05$, cluster corrected).

and thalamus. During delay, load-sensitive regions included bilateral premotor gyri, middle and inferior frontal gyri, and left superior parietal lobule. During the presentation of the probe, there was only one load-sensitive region, located in left middle frontal gyrus.

fMRI Voxelwise Analysis

Voxelwise regressions on load-sensitive voxels during all 3 trial epochs revealed that there were no significant voxels during the cue or probe epochs that correlated with either caudate or putamen ROI K_i. During the delay period, however, we identified a correlation between putamen K_i and delay activation located in the right supramarginal gyrus (maximum; 45, −38, 46 mm) (not shown).

Also during the delay period, we identified a significant correlation between caudate K_i and activation in a region at the border of the left middle frontal gyrus and precentral gyrus (maximum; −38, 4, 36 mm). The correlation between caudate K_i

Table 2

Regions showing increased activation with increasing WM load are shown (activation illustrated in Fig. 2)

Brain region	ROI						
	R/L	*x*	*y*	*z*	BA	No. of vox.	*t* Value
Load-sensitive regions							
Cue							
Middle frontal gyrus	L	−26	−4	58	6/8	130	6.75
		−48	40	20	45	75	5.11
Middle frontal gyrus	R	50	−8	52	6/8	304	4.80
		40	44	36	9/46	534	4.11
Inferior frontal gyrus	L	−48	6	28	44	399	4.30
Inferior frontal gyrus	R	48	4	26	44	439	7.15
Superior parietal lobule	L	−22	−68	42	7	1476	8.86
Superior parietal lobule	R	18	−68	58	40/7	1551	7.36
Inferior parietal lobule	L	−24	−68	42	7	431	8.82
		−56	−22	38	7	144	5.61
Inferior parietal lobule	R	28	−50	52	7	558	8.18
Precentral gyrus	L	−52	−2	34	4/6	1758	8.77
Precentral gyrus	R	46	2	32	6	1499	8.58
Supplementary motor area	L	−8	6	46	24/32	880	7.96
Supplementary motor area	R	2	8	52	24/32	593	6.99
Caudate	L	−12	16	−2		21	3.98
Caudate	R	22	20	14		28	4.30
Putamen	L	−24	10	8		312	5.35
Putamen	R	24	4	10		260	6.31
Thalamus	L	−14	−16	12		511	6.74
Thalamus	R	12	−10	8		562	6.20
Occipital cortex	L	−22	−68	30	18/19	2811	10.5
Occipital cortex	R	22	−62	34	18/19	2085	8.69
Delay							
Middle frontal gyrus	L	−48	6	52	6/9	39	4.51
		−52	12	44	6/9	19	3.96
Middle frontal gyrus	R	36	34	36	46	167	6.30
		44	6	38	6/44	141	5.10
Inferior frontal gyrus	L	−52	14	28	44	249	5.37
Inferior frontal gyrus	R	38	4	34	44	22	4.50
Inferior parietal lobule	L	−28	−62	40	7	43	4.62
Inferior parietal lobule	R	48	−42	46	40	102	4.42
Superior parietal lobule	L	−26	−60	44	7	132	4.27
Precentral gyrus	L	−54	−2	44	6	708	6.24
Precentral gyrus	R	48	0	34	4/6	356	6.39
Supplementary motor area	L	−6	6	54	6/32	142	4.62
Supplementary motor area	R	2	12	52	32	6	3.84
Probe							
Middle frontal gyrus	L	−42	4	54	9/46	200	4.15

Note: Listed for each region is the peak coordinate with respect to the MNI template, number of voxels within the cluster of activation within an anatomically distinct region, the Broadmann Area (BA) of the peak, and the *t*-value of the load effect for the peak (see Methods).

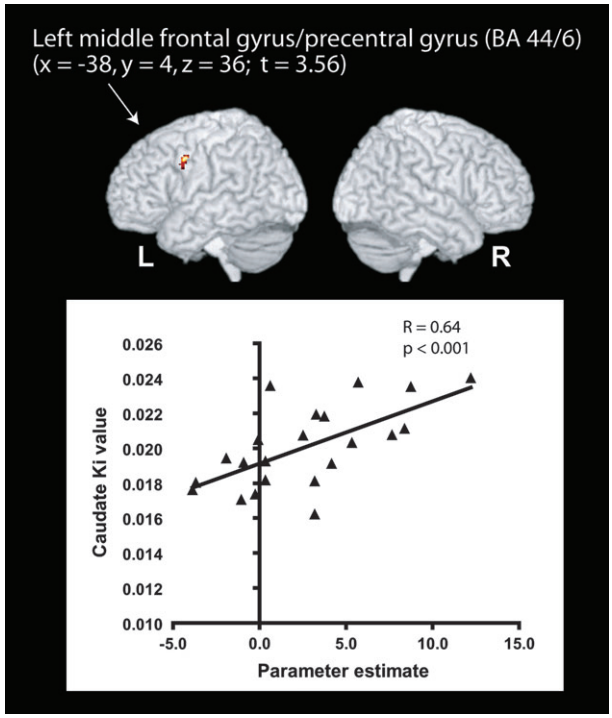

Figure 3. Higher caudate ROI K_i is associated with both increased frontal delay-period activation. A voxelwise regression on fMRI activation during the delay (restricted to the load-sensitive delay-period voxels only, shown in Fig. 2 and listed in Table 2) and caudate K_i values revealed a region in the left middle frontal gyrus/precentral gyrus (IFJ) where these factors were significantly correlated ($P < 0.001$, uncorrected). A scatter plot of the correlation between caudate K_i values and mean parameter estimates in this region is shown. For display purposes, the region is shown including contiguous suprathreshold voxels outside of the map of only load-sensitive voxels that were significant at clusterwise $P < 0.05$.

and mean parameter estimates in this region for each individual is shown in Figure 3. This region overlaps with the inferior frontal junction (IFJ), which lies posterior to the mid-dorsolateral PFC at the intersection of inferior frontal sulcus and the inferior precentral sulcus (Brass et al. 2005). A follow-up analysis also showed that the mean parameter estimates for this region correlated positively with mean task accuracy ($R = 0.64$, $P < 0.05$).

Discussion

This study reports that variability in striatal dopamine function is linked to both WM capacity and brain activation during WM maintenance in older individuals. In particular, ROI and voxelwise analyses of PET data revealed that caudate dopamine function is correlated with WM capacity. Putamen dopamine, in contrast, correlated with motor speed but not WM performance. With respect to our fMRI results, we observed significant relationships between brain activation and dopamine function only during the delay epoch of the WM task, and not the cue or probe. Specifically, we found that activation related to increased WM load in a left IFJ region correlated with caudate dopamine ROI K_i and Sternberg task accuracy. Also during the delay, activation in a right supramarginal gyrus region correlated with putamen dopamine.

Taken together, the relationships between all 3 factors (striatal dopamine, WM performance, and brain activation related to WM maintenance) suggest that caudate dopamine function plays a unique role in mediating WM capacity and load-dependent PFC activation.

The association between caudate dopamine and WM capacity is congruent with our fMRI results, which show that caudate dopamine was associated with activation in the inferior frontal gyrus during WM maintenance. The maintenance processes and motor preparation processes required during the delay epoch of WM tasks are thought to be more dependent on dopamine function than other WM processes (Goldman-Rakic 1996). Maintenance processing under high-load demand is also likely a key component of the complex set skills required for the Listening Span Test, which would explain why caudate dopamine correlated with both maintenance-related activation and performance on this task.

Our findings are consistent with previous studies that have reported correlations between dopamine function and measures of cognitive and motor performance in healthy aging (Volkow et al. 1998; Erixon-Lindroth et al. 2005) and young subjects (Kimberg et al. 1997, 2001), along with recent data

supporting a relationship between WM capacity and dopamine synthesis capacity in young adults (Cools et al. 2008). Our behavioral results are also in agreement with previous studies and existing conceptualizations of separate roles for caudate and putamen in motor and cognitive functions, respectively. Our finding that WM capacity (and, marginally, recognition accuracy) is related to caudate K_i, whereas motor speed is related only to putamen K_i agrees with data from studies of PD patients (Rubin 1999; Rinne et al. 2000; Bruck et al. 2001), patients with striatal lesions (Bhatia and Marsden 1994), and fMRI studies of activation in healthy subjects as well (Lewis et al. 2004). In addition, this pattern is consistent with the functional organization of basal ganglia–thalamocortical loops in which pathways are segregated into motor and dorsolateral PFC or "cognitive" circuits involving putamen and caudate, respectively (Alexander et al. 1986). Our data also show that caudate dopamine is related with some topographic specificity to delay-period activation in PFC, in the left IFJ, to which it is reciprocally linked (Lehericy et al. 2004) (Fig. 3).

Putamen dopamine, on the other hand, correlated with maintenance-related activation in the supramarginal gyrus, just posterior to the postcentral gyrus. Based on our behavioral results, we predicted that putamen dopamine would correlate primarily with activation in regions that participate in motor or motor preparation. However, the right supramarginal gyrus activation we observed is posterior to these regions, in the inferior parietal lobule, a multimodal region that is involved in the integration of visual and sensorimotor information, and is frequently coactivated with PFC during WM paradigms (Wager and Smith 2003).

The neuroimaging data thus do not support a strict dissociation for the roles of caudate and putamen with cognitive and motor functions, respectively, but instead provide evidence that both caudate and putamen dopamine contribute to cognitive aspects of the task. Thus dopaminergic neurotransmission within caudate and putamen nigrostriatal circuits may jointly influence WM function because of some degree of functional integration (Haber 2003). Through the integration of these nigrostriatal circuits, dopaminergic changes that influence the PFC will also lead to changes in parietal regions as well. Supporting this idea are recent FDG PET studies which report that inferior and posterior parietal regions are part of a network including the PFC that shows reduced glucose metabolism that parallels disease progression (Huang, Tang, et al. 2007) and executive function deficits (Huang, Mattis, et al. 2007) in Parkinson's disease patients. This concept of the joint influence of caudate and putamen dopamine on WM is also consistent with the nonsignificant correlation trend we found between WM capacity and putamen dopamine ($P = 0.12$; see Table 1) and with the findings of Chang et al. (2007), who reported bilateral dorsal putamen load-related BOLD activation during the encoding and maintenance phases of a very similar task (Chang et al. 2007). Finally, another explanation that is compatible with these ideas is that because the maintenance period involves motor preparation as well as WM maintenance, the supramarginal gyrus activation that correlates with putamen dopamine may reflect engagement of attentional processes required specifically for the *motor* preparation of the upcoming response.

Although the mesocortical dopamine system has previously been thought to support WM function through innervation of the PFC, our results support a specific role for the nigrostriatal dopaminergic system in this cognitive process. This role is consistent with results obtained in PD patients (Owen et al. 1998; Mattay et al. 2002; Lewis et al. 2003; Monchi et al. 2004) and normal subjects (Owen et al. 1996; Chang et al. 2007). In a recent study that also used the Sternberg task and an event-related fMRI design (Chang et al. 2007), load-related patterns of both basal ganglia and cortical activation were similar to those reported here. Interestingly, this study also employed a connectivity analysis to show associations between striatal and cortical activity during the maintenance phase of this task, supporting a role for basal ganglia–PFC interactions during WM maintenance. Both our study and Chang et al. reported bilateral load-related activation of the striatum during performance of this task, which supports the idea that putamen, as well as caudate, contributes to the cognitive aspects of the task. We observed this load-related activation during the encoding period, as opposed to the delay period as also observed by Chang et al. which we would have predicted because we observed the correlations with dopamine variability. The fact that we did not observe striatal activity during the delay may be due to differences in statistical thresholding used in our study compared with that of Chang et al. Nonetheless, these findings provide support for the idea that dopamine release is associated with increased BOLD signal (Knutson and Gibbs 2007). Our data extend these findings by providing support for a relationship between striatal dopaminergic function, behavior, and PFC activity that is most pronounced during the delay period of this task. We report here that improved cognition is associated with greater dopaminergic function and *more* cortical activation, findings that support the idea of increased activation in healthy aging that provides a compensatory role and underlies successful performance (Cabeza 2002; Cabeza et al. 2002).

The anatomy and physiology of the basal ganglia–thalamocortical circuits provide a mechanism that may account for these findings. Through its inhibitory action via the "direct" pathway (Parent and Lavoie 1993), striatal dopamine should reduce inhibitory pallidal outflow to the thalamus and thereby excite cortex. This idea has been supported by observations of altered pallidal outflow in PD patients (Owen et al. 1992) and increased brain activation in motor cortex with dopaminergic treatment of PD patients (Jenkins et al. 1992; Rascol et al. 1994; Sabatini et al. 2000; Mattay et al. 2002). Electrophysiological studies in primates demonstrate increased firing rates in both caudate (Hikosaka et al. 1989) and thalamus (Fuster and Alexander 1973) during the delay period of a delayed-response task, and decreased firing rates in globus pallidus (Mushiake and Strick 1995). These data have prompted computational models of WM in which the striatum plays an active role in maintenance through pallido-thalamocortical projections that sustain activity in PFC (Monchi et al. 2000; Frank et al. 2001; Ashby et al. 2005; Gruber et al. 2006). Our data thus support a model in which striatal dopamine plays a key role in WM maintenance and cortical excitation.

Although striatal dopamine function appears to play an important role in this WM task, the PFC is critically involved as well. The left PFC, in particular, appears to play several roles that are relevant to the interpretation of our results. Load-related fMRI activation in the left inferior frontal gyrus has been observed previously for this task (Awh et al. 1996; Altamura et al. 2007) and may be related to subvocal rehearsal. There is a great deal of evidence that PFC activation increases when WM

demand is high (Hester and Garavan 2004). This data, in conjunction with studies reporting changes in PFC activation that are associated with responses to dopaminergic medication (Gibbs and D'Esposito 2005), provide support for our findings that the influence of dopamine on PFC function is most apparent under high-load conditions.

The IFJ is a region receiving recent attention for its role in cognitive control (Brass et al. 2005), a process that is also strongly associated with dopamine function and the PFC (Braver and Cohen 2000a). The IFJ is located just posterior to the ventral PFC, at the junction of premotor, language, and WM domains, and is known to be activated in tasks that require the unification of these domains (Brass et al. 2005). In particular, the peak coordinates of a region found to increase activation in parallel with increased WM load during a task similar to ours were very close to the region we report here (Hester and Garavan 2004). Furthermore, a recent meta-analysis identified the IFJ as a critical region for a number of tasks whose common theme was updating abstract task representations following a cue (Derrfuss et al. 2005). This is entirely consistent with our observation of activation in this region, in that both WM maintenance and high-load conditions are situations requiring updating of abstract task representations.

A critical feature of the IFJ region we identified was that it correlated with caudate dopamine function and task accuracy (Fig. 3), suggesting that it is a candidate site for the integration of to-be-remembered information with preparation of the motor response. Dopaminergic transmission may be particularly important during WM maintenance because it is during this period that subjects maintain the cue stimulus in WM and prepare for the appearance of the probe stimulus and the subsequent motor response. This period requires both stimulus maintenance and motor preparation, the integration of which is associated with activation the IFJ. Thus our data provides evidence that this integrative role of the IFJ may, in addition, depend on dopamine function in the caudate.

Several additional points related to the interpretation of these findings also deserve comment. First, an important distinction between our 2 neuroimaging measures was that our PET data represent a static measure of dopamine synthesis occurring over long times, whereas our fMRI data represent a dynamic measure of brain activation.

Second, it is important to note that the associations we observed between striatal dopamine and PFC function do not indicate which factor plays the causal role. Although the most obvious explanation is that variability in dopamine levels influences PFC function via the nigrostriatal circuit as described above, the effects we observed could also be explained by increased input from frontal regions to the striatum. Within the nigrostriatal circuit, there is glutamatergic feedback frontal regions to the anterior caudate and putamen (Pycock et al. 1980; Parent and Hazrati 1995), and this pathway has been shown to induce dopamine release in the striatum using repetitive transcranial magnetic stimulation of the dorsolateral PFC (Strafella et al. 2001). Finally, our study does not compare young and old subjects and therefore does not address possible differences in dopamine function or PFC activity across the lifespan. Although we found no evidence for an effect of age on dopamine synthesis, it is possible that age-related processes contributed to the variability in both dopamine and brain activation. The tracer FMT is an index of AADC activity, which appears to remain stable or show only slight decreases with age (Kish et al. 1992) that are disproportionate to the marked decreases in dopamine transporters (Volkow et al. 1996; Erixon-Lindroth et al. 2005) and receptors (Volkow et al. 2000) in normal aging. These findings, in conjunction with studies in rodents which have reported increases in AADC activity following treatments that decrease dopaminergic transmission (Zhu et al. 1992; Young et al. 1993) suggest that successful WM processing in aging may involve preservation or upregulation of the dopamine-mediated nigrostriatal pathway, although this idea is not proven (Haycock et al. 2003).

Although these data provide support for the role of striatal dopamine in WM capacity and maintenance, many questions about the specific role of these structures as well as the pharmacology of the effect require exploration. For example, it is unclear exactly how the striatum is involved in maintenance, and whether its function is also related to the proposed role that this structure may play in both gating and updating representations. Our data suggest that a major role may be to integrate maintenance and motor preparation. As we have examined dopamine synthesis capacity, the relative contribution of D1 and D2 receptor families is also unknown. Finally, the considerable evidence implicating PFC dopamine in WM function suggests that the mesocortical and nigrostriatal dopamine systems must work together in carrying out this cognitive task although the nature of this interaction is unknown.

Funding

National Institute on Aging grant (AG027984).

Notes

We thank Cindee Madison, Lieke Wiggers, Michael Oliver, Dawn Chen, Felice Sun, Sasha Gibbs, Jamie Eberling, Roshan Cools, and Mark D'Esposito for helpful comments and contributions this manuscript. *Conflict of Interest*: None declared.

Address correspondence to Susan M. Landau, PhD, Helen Wills Neuroscience Institute, 132 Barker Hall #3190, Berkeley, CA 94720-3192. Email: slandau@berkeley.edu.

References

Alexander GE, Crutcher MD. 1990. Functional architecture of basal ganglia circuits: neural substrates of parallel processing. Trends Neurosci. 13:266–271.

Alexander GE, DeLong MR, Strick PL. 1986. Parallel organization of functionally segregated circuits linking basal ganglia and cortex. Annu Rev Neurosci. 9:357–381.

Altamura M, Elvevag B, Blasi G, Bertolino A, Callicott JH, Weinberger DR, Mattay VS, Goldberg TE. 2007. Dissociating the effects of Sternberg working memory demands in prefrontal cortex. Psychiatry Res. 154:103–114.

Ashby FG, Ell SW, Valentin VV, Casale MB. 2005. FROST: a distributed neurocomputational model of working memory maintenance. J Cogn Neurosci. 17:1728–1743.

Awh E, Jonides J, Smith EE, Schumacher EH, Koeppe RA, Katz S. 1996. Dissociation of storage and rehearsal in verbal working memory. Psychol Sci. 7:25–31.

Backman L, Ginovart N, Dixon RA, Wahlin TB, Wahlin A, Halldin C, Farde L. 2000. Age-related cognitive deficits mediated by changes in the striatal dopamine system. Am J Psychiatry. 157:635–637.

Baddeley A. 1992. Working memory. Science. 255:556–559.

Bhatia KP, Marsden CD. 1994. The behavioural and motor consequences of focal lesions of the basal ganglia in man. Brain. 117(Pt 4): 859–876.

Brass M, Derrfuss J, Forstmann B, von Cramon DY. 2005. The role of the inferior frontal junction area in cognitive control. Trends Cogn Sci. 9:314–316.

Braver TS, Cohen JD. 2000a. The control of control: the role of dopamine in regulating prefrontal function and working memory. In: Monsell S, Driver J, editors. Control of cognitive processes: attention and performance 18. Cambridge: Massachusetts Institute of Technology Press. p. 713–737.

Bruck A, Portin R, Lindell A, Laihinen A, Bergman J, Haaparanta M, Solin O, Rinne JO. 2001. Positron emission tomography shows that impaired frontal lobe functioning in Parkinson's disease is related to dopaminergic hypofunction in the caudate nucleus. Neurosci Lett. 311:81–84.

Cabeza R. 2002. Hemispheric asymmetry reduction in older adults: the HAROLD model. Psychol Aging. 17:85–100.

Cabeza R, Anderson ND, Locantore JK, McIntosh AR. 2002. Aging gracefully: compensatory brain activity in high-performing older adults. Neuroimage. 17:1394–1402.

Cao J. 1999. The size of the connected components of excursion sets of X2, t, and F fields. Adv Appl Probab. 31:577–594.

Carbon M, Ma Y, Barnes A, Dhawan V, Chaly T, Ghilardi MF, Eidelberg D. 2004. Caudate nucleus: influence of dopaminergic input on sequence learning and brain activation in Parkinsonism. Neuroimage. 21:1497–1507.

Chang C, Crottaz-Herbette S, Menon V. 2007. Temporal dynamics of basal ganglia response and connectivity during verbal working memory. Neuroimage. 34:1253–1269.

Cools R, Gibbs SE, Miyakawa A, Jagust W, D'Esposito M. 2008. Working memory capacity predicts dopamine synthesis capacity in the human striatum. J Neurosci. 28:1208–1212.

Cools R, Robbins TW. 2004. Chemistry of the adaptive mind. Philos Trans A Math Phys Eng Sci. 362:2871–2888.

DeJesus OT. 2003. Positron-labeled DOPA analogs to image dopamine terminals. Drug Dev Res. 59:249–260.

DeJesus OT, Endres CJ, Shelton SE, Nickles RJ, Holden JE. 1997. Evaluation of fluorinated m-tyrosine analogs as PET imaging agents of dopamine nerve terminals: comparison with 6-fluoroDOPA. J Nucl Med. 38:630–636.

Durstewitz D, Seamans JK. 2002. The computational role of dopamine D1 receptors in working memory. Neural Netw. 15:561–572.

Erixon-Lindroth N, Farde L, Wahlin TB, Sovago J, Halldin C, Backman L. 2005. The role of the striatal dopamine transporter in cognitive aging. Psychiatry Res. 138:1–12.

Esaki T, Itoh Y, Shimoji K, Cook M, Jehle J, Sokoloff L. 2002. Effects of dopamine receptor blockade on cerebral blood flow response to somatosensory stimulation in the unanesthetized rat. J Pharmacol Exp Ther. 303:497–502.

Fahn S, Elton RI, editors. UPDRS Development Committee: Unified Parkinson's Rating Scale. Florham Park (NJ): MacMillan Healthcare Information.

Floresco SB, Phillips AG. 2001. Delay-dependent modulation of memory retrieval by infusion of a dopamine D1 agonist into the rat medial prefrontal cortex. Behav Neurosci. 115:934–939.

Folstein MF, Folstein SE, McHugh PR. 1975. "Mini-mental state". A practical method for grading the cognitive state of patients for the clinician. J Psychiatr Res. 12:189–198.

Frank MJ, Loughry B, O'Reilly RC. 2001. Interactions between frontal cortex and basal ganglia in working memory: a computational model. Cogn Affect Behav Neurosci. 1:137–160.

Fuster JM, Alexander GE. 1973. Firing changes in cells of the nucleus medialis dorsalis associated with delayed response behavior. Brain Res. 61:79–91.

Gibbs SE, D'Esposito M. 2005. Individual capacity differences predict working memory performance and prefrontal activity following dopamine receptor stimulation. Cogn Affect Behav Neurosci. 5:212–221.

Goldman-Rakic PS. 1996. Regional and cellular fractionation of working memory. Proc Natl Acad Sci USA. 93:13473–13480.

Gruber AJ, Dayan P, Gutkin BS, Solla SA. 2006. Dopamine modulation in the basal ganglia locks the gate to working memory. J Comput Neurosci. 20:153–166.

Haber SN. 2003. The primate basal ganglia: parallel and integrative networks. J Chem Neuroanat. 26:317–330.

Haycock JW, Becker L, Ang L, Furukawa Y, Hornykiewicz O, Kish SJ. 2003. Marked disparity between age-related changes in dopamine and other presynaptic dopaminergic markers in human striatum. J Neurochem. 87:574–585.

Hester R, Garavan H. 2004. Executive dysfunction in cocaine addiction: evidence for discordant frontal, cingulate, and cerebellar activity. J Neurosci. 24:11017–11022.

Hikosaka O, Sakamoto M, Sadanari U. 1989. Functional properties of monkey caudate neurons 3: Activities related to expectation of target and reward. J Neurophysiol. 61:814–831.

Huang C, Mattis P, Tang C, Perrine K, Carbon M, Eidelberg D. 2007. Metabolic brain networks associated with cognitive function in Parkinson's disease. Neuroimage. 34:714–723.

Huang C, Tang C, Feigin A, Lesser M, Ma Y, Pourfar M, Dhawan V, Eidelberg D. 2007. Changes in network activity with the progression of Parkinson's disease. Brain. 130:1834–1846.

Jenkins IH, Fernandez W, Playford ED, Lees AJ, Frackowiak RS, Passingham RE, Brooks DJ. 1992. Impaired activation of the supplementary motor area in Parkinson's disease is reversed when akinesia is treated with apomorphine. Ann Neurol. 32:749–757.

Jordan S, Eberling JL, Bankiewicz KS, Rosenberg D, Coxson PG, VanBrocklin HF, O'Neil JP, Emborg ME, Jagust WJ. 1997. 6-[18F]fluoro-L-m-tyrosine: metabolism, positron emission tomography kinetics, and 1-methyl-4-phenyl-1,2,3,6-tetrahydropyridine lesions in primates. Brain Res. 750:264–276.

Kimberg DY, Aguirre GK, Lease J, D'Esposito M. 2001. Cortical effects of bromocriptine, a D-2 dopamine receptor agonist, in human subjects, revealed by fMRI. Hum Brain Mapp. 12:246–257.

Kimberg DY, D'Esposito M, Farah MJ. 1997. Effects of bromocriptine on human subjects depend on working memory capacity. Neuroreport. 8:3581–3585.

Kish SJ, Shannak K, Rajput A, Deck JH, Hornykiewicz O. 1992. Aging produces a specific pattern of striatal dopamine loss: implications for the etiology of idiopathic Parkinson's disease. J Neurochem. 58:642–648.

Klein GJ, Teng X, Jagust WJ, Eberling JL, Acharya A, Reutter BW, Huesman RH. 1997. A methodology for specifying PET VOI's using multimodality techniques. IEEE Trans Med Imaging. 16:405–415.

Knutson B, Gibbs SE. 2007. Linking nucleus accumbens dopamine and blood oxygenation. Psychopharmacology (Berl). 191:813–822.

Kochunov P, Lancaster JL, Thompson P, Woods R, Mazziotta J, Hardies J, Fox P. 2001. Regional spatial normalization: toward an optimal target. J Comput Assist Tomogr. 25:805–816.

Krimer LS, Muly EC, 3rd, Williams GV, Goldman-Rakic PS. 1998. Dopaminergic regulation of cerebral cortical microcirculation. Nat Neurosci. 1:286–289.

Lammertsma AA, Hume SP. 1996. Simplified reference tissue model for PET receptor studies. Neuroimage. 4:153–158.

Lehericy S, Ducros M, Van de Moortele PF, Francois C, Thivard L, Poupon C, Swindale N, Ugurbil K, Kim DS. 2004. Diffusion tensor fiber tracking shows distinct corticostriatal circuits in humans. Ann Neurol. 55:522–529.

Lewis SJ, Dove A, Robbins TW, Barker RA, Owen AM. 2003. Cognitive impairments in early Parkinson's disease are accompanied by reductions in activity in frontostriatal neural circuitry. J Neurosci. 23:6351–6356.

Lewis SJ, Dove A, Robbins TW, Barker RA, Owen AM. 2004. Striatal contributions to working memory: a functional magnetic resonance imaging study in humans. Eur J Neurosci. 19:755–760.

Mattay VS, Tessitore A, Callicott JH, Bertolino A, Goldberg TE, Chase TN, Hyde TM, Weinberger DR. 2002. Dopaminergic modulation of cortical function in patients with Parkinson's disease. Ann Neurol. 51:156–164.

Middleton FA, Strick PL. 2000. Basal ganglia and cerebellar loops: motor and cognitive circuits. Brain Res Brain Res Rev. 31:236–250.

Monchi O, Petrides M, Doyon J, Postuma RB, Worsley K, Dagher A. 2004. Neural bases of set-shifting deficits in Parkinson's disease. J Neurosci. 24:702–710.

Monchi O, Taylor JG, Dagher A. 2000. A neural model of working memory processes in normal subjects, Parkinson's disease, and schizophrenia for fMRI design and predictions. Neural Netw. 13:953–973.

Mushiake H, Strick PL. 1995. Pallidal neuron activity during sequential arm movements. J Neurophysiol. 74:2754–2758.

Namavari M, Satyamurthy N, Phelps ME, Barrio JR. 1993. Synthesis of 6-[18F] and 4-[18F]fluoro-L-m-tyrosines via regioselective radiofluorodestannylation. Appl Radiat Isot. 44:527–536.

Owen AM, Doyon J, Dagher A, Sadikot A, Evans AC. 1998. Abnormal basal ganglia outflow in Parkinson's disease identified with PET. Implications for higher cortical functions. Brain. 121(Pt 5):949–965.

Owen AM, Doyon J, Petrides M, Evans AC. 1996. Planning and spatial working memory: a positron emission tomography study in humans. Eur J Neurosci. 8:353–364.

Owen AM, James M, Leigh PN, Summers BA, Marsden CD, Quinn NP, Lange KW, Robbins TW. 1992. Fronto-striatal cognitive deficits at different stages of Parkinson's disease. Brain. 115(Pt 6):1727–1751.

Parent A, Hazrati LN. 1995. Functional anatomy of the basal ganglia 1: The cortico-basal ganglia-thalamo-cortical loop. Brain Res Brain Res Rev. 20:91–127.

Parent A, Lavoie B. 1993. The heterogeneity of the mesostriatal dopaminergic system as revealed in normal and parkinsonian monkeys. Adv Neurol. 60:25–33.

Patlak CS, Blasberg RG. 1985. Graphical evaluation of blood-to-brain transfer constants from multiple-time uptake data. Generalizations. J Cereb Blood Flow Metab. 5:584–590.

Pycock CJ, Carter CJ, Kerwin RW. 1980. Effect of 6-hydroxydopamine lesions of the medial prefrontal cortex on neurotransmitter systems in subcortical sites in the rat. J Neurochem. 34:91–99.

Rascol O, Sabatini U, Chollet F, Fabre N, Senard JM, Montastruc JL, Celsis P, Marc-Vergnes JP, Rascol A. 1994. Normal activation of the supplementary motor area in patients with Parkinson's disease undergoing long-term treatment with levodopa. J Neurol Neurosurg Psychiatry. 57:567–571.

Reuter-Lorenz PA, Lustig C. 2005. Brain aging: reorganizing discoveries about the aging mind. Curr Opin Neurobiol. 15:245–251.

Rinne JO, Portin R, Ruottinen H, Nurmi E, Bergman J, Haaparanta M, Solin O. 2000. Cognitive impairment and the brain dopaminergic system in Parkinson disease: [18F]fluorodopa positron emission tomographic study. Arch Neurol. 57:470–475.

Rubin DC. 1999. Frontal-striatal circuits in cognitive aging: evidence for caudate involvement. Aging Neuropsychol Cognit. 6:241–259.

Rypma B, Berger JS, D'Esposito M. 2002. The influence of working-memory demand and subject performance on prefrontal cortical activity. J Cogn Neurosci. 14:721–731.

Sabatini U, Boulanouar K, Fabre N, Martin F, Carel C, Colonnese C, Bozzao L, Berry I, Montastruc JL, Chollet F, Rascol O. 2000. Cortical motor reorganization in akinetic patients with Parkinson's disease: a functional MRI study. Brain. 123(Pt 2):394–403.

Salthouse TA, Babcock RL, Shaw RJ. 1991. Effects of adult age on structural and operational capacities in working memory. Psychol Aging. 6:118–127.

Schultz W, Apicella P, Ljungberg T. 1993. Responses of monkey dopaminergic neurons to reward and conditioned stimuli during successive steps of learning a delayed response task. J Neurosci. 13:900–913.

Sternberg S. 1966. High-speed scanning in human memory. Science. 153:652–654.

Strafella AP, Paus T, Barrett J, Dagher A. 2001. Repetitive transcranial magnetic stimulation of the human prefrontal cortex induces dopamine release in the caudate nucleus. J Neurosci. 21:RC157.

Vijayraghavan S, Wang M, Birnbaum SG, Williams GV, Arnsten AF. 2007. Inverted-U dopamine D1 receptor actions on prefrontal neurons engaged in working memory. Nat Neurosci. 10:376–384.

Volkow ND, Ding YS, Fowler JS, Wang GJ, Logan J, Gatley SJ, Hitzemann R, Smith G, Fields SD, Gur R. 1996. Dopamine transporters decrease with age. J Nucl Med. 37:554–559.

Volkow ND, Gur RC, Wang GJ, Fowler JS, Moberg PJ, Ding YS, Hitzemann R, Smith G, Logan J. 1998. Association between decline in brain dopamine activity with age and cognitive and motor impairment in healthy individuals. Am J Psychiatry. 155:344–349.

Volkow ND, Logan J, Fowler JS, Wang GJ, Gur RC, Wong C, Felder C, Gatley SJ, Ding YS, Hitzemann R, Pappas N. 2000. Association between age-related decline in brain dopamine activity and impairment in frontal and cingulate metabolism. Am J Psychiatry. 157:75–80.

Wager TD, Smith EE. 2003. Neuroimaging studies of working memory: a meta-analysis. Cogn Affect Behav Neurosci. 3:255–274.

Wang GJ, Volkow ND, Levy AV, Fowler JS, Logan J, Alexoff D, Hitzemann RJ, Schyler DJ. 1996. MR-PET image coregistration for quantitation of striatal dopamine D2 receptors. J Comput Assist Tomogr. 20:423–428.

Wechsler D. 1987. Wechsler Memory Scale—Revised, manual. San Antonio: The Psychological Corporation.

Williams GV, Goldman-Rakic PS. 1995. Modulation of memory fields by dopamine D1 receptors in prefrontal cortex. Nature. 376: 572–575.

Worsley KJ, Friston KJ. 1995. Analysis of fMRI time-series revisited—again. Neuroimage. 2:173–181.

Yesavage JA, Brink TL, Rose TL, Lum O, Huang V, Adey M, Leirer VO. 1982–1983. Development and validation of a geriatric depression rating scale: a preliminary report. J Psychiatr Res. 17:37–49.

Young EA, Neff NH, Hadjiconstantinou M. 1993. Evidence for cyclic AMP-mediated increase of aromatic L-amino acid decarboxylase activity in the striatum and midbrain. J Neurochem. 60: 2331–2333.

Zarahn E, Aguirre GK, D'Esposito M. 1999. Temporal isolation of the neural correlates of spatial mnemonic processing with fMRI. Brain Res Cogn Brain Res. 7:255–268.

Zhu MY, Juorio AV, Paterson IA, Boulton AA. 1992. Regulation of aromatic L-amino acid decarboxylase by dopamine receptors in the rat brain. J Neurochem. 58:636–641.